

# VITAGRAPH: Building a Knowledge Graph for Biologically Relevant Learning Tasks

**Francesco Madeddu\***

DIAG, Sapienza University of Rome  
IAC, CNR Consiglio Nazionale delle Ricerche  
madeddu@diag.uniroma1.it

**Lucia Testa\***

DIAG, Sapienza University of Rome  
lucia.testa@uniroma1.it

**Gianluca De Carlo\*†**

DIAG, Sapienza University of Rome  
decarlo@diag.uniroma1.it

**Michele Pieroni**

Department of Biochemical Sciences  
Sapienza University of Rome  
mi.pieroni@uniroma1.it

**Andrea Mastropietro**

Department of Life Science Informatics and  
Data Science, University of Bonn and Lamarr Institute  
mastropietro@bit.uni-bonn.de

**Aris Anagnostopoulos**

DIAG, Sapienza University of Rome  
aris.@diag.uniroma1.it

**Paolo Tieri**

IAC, CNR Consiglio Nazionale delle Ricerche  
paolo.tieri@cnr.it

**Sergio Barbarossa**

DIET, Sapienza University of Rome  
sergio.barbarossa@uniroma1.it

## Abstract

The intrinsic complexity of human biology presents ongoing challenges to scientific understanding. Researchers worldwide collaborate across disciplines to expand our knowledge of the biological interactions that define human life. Artificial intelligence (AI) methodologies have emerged as powerful tools across scientific domains, particularly in computational biology, where graph data structures effectively model biological entities such as protein–protein interaction (PPI) networks and gene functional networks. Those networks are used as datasets for paramount network medicine tasks, such as gene–disease association prediction, drug repurposing, and polypharmacy side effect studies. Reliable predictions from machine learning models require high-quality foundational data. In this work, we present a comprehensive multi-purpose biological knowledge graph constructed by integrating and refining multiple publicly available datasets. Building upon the Drug Repurposing Knowledge Graph (DRKG), we define an advanced pipeline tasked with a) cleaning inconsistencies and redundancies present in DRKG, b) coalescing information from the main available public data sources, and c) enriching the graph nodes with expressive feature vectors such as molecular fingerprints and gene ontologies, among others. Biologically and chemically relevant features improve the capacity of machine learning models to generate accurate and well-structured embedding spaces.

\*Those authors contributed equally.

†Work done while the author was on a short-term visit at University of Cambridge, UK.

The resulting resource represents a coherent and reliable biological knowledge graph that serves as a state-of-the-art platform to advance research in computational biology and precision medicine. Moreover, it offers the opportunity to benchmark graph-based machine learning and network medicine models on relevant tasks. We demonstrate the effectiveness of the proposed dataset by benchmarking it against the task of drug repurposing, PPI predictions, and side-effect predictions, modeled as link prediction problems. Our dataset, VITAGRAPH, is available at: <https://www.kaggle.com/datasets/gianlucadecarlods/vitagraph/>.

## 1 Introduction

Bioinformatics has undergone remarkable advancements in recent years [1]. This field aims to elucidate complex biological phenomena through the analysis of biological data. Of particular interest are omics data [2, 3]. The latter encompass molecular information and the interactions among biomolecules across various levels, including genomics, proteomics, and transcriptomics. Notably, the growing interest in understanding protein interactions within organisms has led to the concept of interactome, which involves the construction and analysis of networks representing biological entities and interactions among them. In this context, network medicine [4] has emerged as a powerful approach for addressing biologically relevant problems by exploiting the structural information encoded in biological networks. One of the most prominent and widely utilized types of such networks is the protein–protein interaction (PPI) network [5]. In these networks, nodes represent genes or proteins, and edges denote physical interactions. PPI networks, such as BioGRID [5], STRING [6], and HuRI [7], have been extensively employed, yielding promising results in various applications, including the identification of gene–disease associations (GDAs) [8–10] and the prediction of novel protein–protein interactions [11]. Other relevant types of biological networks include gene regulatory networks [12], in which nodes representing genes are connected based on their involvement in regulating gene expression, ultimately influencing cellular function. These networks provide complementary information to that offered by PPI networks. Gene–disease networks, typically modeled as bipartite graphs, represent associations between genes and diseases; an edge exists if a gene is implicated in the etiology or pathophysiological mechanisms of a given disease. A relevant example of such a dataset is given by DisGeNET [13, 14]. Additional relevant types of biomedical networks include drug–drug interaction networks [15], drug–disease networks [16], and drug–side effect networks, exemplified by resources such as SIDER [17] and OffSides [18].

Considered individually, these networks—while well-suited to the specific tasks for which they were designed—are insufficient to capture the full complexity of biological systems. Consequently, biological knowledge graphs have been developed with the aim of integrating and harmonizing diverse types of biological information into a unified data resource [19, 20] that can better model the complexity of biological organisms. A notable effort in the field of biomedical knowledge graphs is represented by the Drug Repurposing Knowledge Graph (DRKG) [21]. Originally developed with the aim of identifying potential drug candidates for treating COVID-19 [22, 23], DRKG integrates a wide range of biomedical data sources. Due to the breadth and diversity of its integrated information, its applicability could be, in principle, extended beyond drug repurposing to a broad range of biologically relevant tasks that can be framed as link prediction problems within the graph learning paradigm.

Despite its potential, the current version of DRKG suffers from numerous inconsistencies that hinder its practical usability and often result in ambiguous or meaningless outcomes. Motivated by the potential offered, we adopted DRKG as the foundation for constructing our proposed knowledge graph. Following a careful and comprehensive cleaning process to address these inconsistencies, we enriched the graph with additional information sourced from reliable and domain-specific biomedical databases. Furthermore, we incorporated biochemically meaningful node features to enhance the expressiveness and biological relevance of the embedded knowledge. We thus propose VITAGRAPH (from the Latin word *vita*, meaning *life*), a novel and versatile knowledge graph tailored for a wide range of biological tasks formulated as link prediction problems, including, but not limited to, drug repurposing, gene–disease association, PPI prediction, and side–effect identification. We propose VITAGRAPH as a robust benchmark for assessing link prediction methodologies in the context of network medicine. We also provide a customizable pipeline to generate the proposed dataset by including or excluding the steps described in the paper, along with code for benchmark purposes.<sup>1</sup>

<sup>1</sup><https://github.com/GiDeCarlo/VitaGraph>

## 2 Rethinking the Drug Repurposing Knowledge Graph

Our dataset is built upon DRKG, a comprehensive and heterogeneous biological network that integrates diverse biomedical entities and their interactions. DRKG encompasses a wide array of entity types, including genes, compounds, diseases, biological processes, side effects, symptoms, and other biologically relevant concepts. Its primary aim is to facilitate the exploration of disease mechanisms at the molecular level and to support drug repositioning efforts. The graph aggregates data from six major biomedical databases: DrugBank [24, 15], Hetionet [25], GNBR [26], STRING [6], IntAct [27], and DGIdb [28, 29], as well as curated information from recent literature, including research related to COVID-19. In its latest release, DRKG comprises 97,238 entities spanning 13 distinct types and contains 5,874,261 triplets distributed across 107 edge types. These edge types capture the various relationships that exist among 17 different entity-type pairs, with multiple interaction types possible between the same entity pairs. For example, a compound may interact with a gene both as an inhibitor and as a binder, while gene–gene interactions may include various regulatory and physical associations. This integration of multiple data sources results in a rich, heterogeneous network structure that offers a robust foundation for modeling complex biological systems. As illustrated in Figure 2a, DRKG consists of multiple node and edge types, with nodes annotated according to their type and source database, and edges representing specific interaction types between node pairs.

The original DRKG comprises a diverse set of node types, including: anatomy (representing human anatomical structures); ATC (the Anatomical Therapeutic Chemical classification system, used by the World Health Organization to classify drugs); biological process, cellular component, and molecular function (the three branches of the Gene Ontology [30], which describe gene functions); compound (chemical molecules); disease; gene; pathway (a sequence of molecular events within cells that drive cellular functions); pharmacologic class (categorizing drug compounds based on pharmacological properties); side effect; symptom; and tax (taxonomic identifiers indicating the species origin of genes, such as human). Comprehensive details on the annotation of nodes and edges are provided in Supplementary Material.

Despite its comprehensive scope, the original DRKG exhibits several shortcomings that limit its usability in downstream tasks. These include the presence of duplicate entries, inconsistent formatting standards, heterogeneous or ambiguous labeling, the inclusion of non-human genes, and invalid or outdated compound identifiers. To address these limitations, a rigorous data cleaning phase was necessary prior to the graph’s integration with additional data sources and the enrichment of nodes with biologically and chemically meaningful features.

### 2.1 Filtering rows with formatting errors

The dataset was analyzed for formatting inconsistencies that could adversely affect downstream processing and analysis. The first issue identified concerned the representation of entity identifiers. While the majority of entries adhered to the format `entity_type:database_source:entity_id`, a subset lacked the database source. To ensure consistency and facilitate the traceability of entity origins, all identifiers were standardized to follow the former format, explicitly indicating the source database.

Secondly, rows containing the semicolon character (“;”) were flagged, as this character often suggested that multiple entities had been erroneously merged into a single node. These inconsistent entries were removed, resulting in the elimination of 1,122 rows.

Thirdly, the dataset included 98 rows in which compounds were separated by the pipe character (“|”). These cases were interpreted as potential formatting errors or ambiguous representations of compound combinations. Due to the uncertainty surrounding their intended semantics and their limited prevalence, these entries were also excluded from the dataset.

### 2.2 Standardization of relationship labels

As previously noted, the original DRKG comprises 107 distinct edge types (interaction types), many of which are expressed using synonymous terms or alternative codes. To reduce redundancy and enhance semantic consistency across the dataset, we performed a harmonization step in which synonymous interaction labels were mapped to a set of unified and standardized terms. This mapping facilitates

more coherent interpretation and analysis of the graph’s relational structure. The complete set of standardized interaction labels and their corresponding original variants is presented in Appendix A.

### 2.3 Removal of non-human information

To focus the dataset on human biology and eliminate biases from COVID-19-related studies, virus-related relationships (e.g., VirGenHumGen, DrugVirGen; see Supplementary Material) were excluded. Non-human genes and their interactions were also removed to avoid introducing noise into human-specific analyses. This filtering step, aimed at enhancing semantic consistency and biological relevance, led to the removal of 135,294 rows and 17,553 non-human genes. For broader research interests, the pipeline allows users to retain non-human interactions by disabling this cleaning step.

### 2.4 Standardization of entity identifiers

The original DRKG was constructed by merging multiple databases that lacked a unified entity identification system, resulting in entities being represented by multiple identifiers. This redundancy led to information loss and fragmentation. To address this issue, we implemented a systematic approach to unify entity identifiers by leveraging supplementary data sources. Mapping entity identifiers poses considerable challenges, particularly because complete cross-database correspondence cannot be ensured, as certain entities may exist exclusively within specific datasets.

**Compound identifier mapping** For the standardization of compound identifiers, we employed the UniChem platform [31], which offers comprehensive cross-referencing services by aggregating information from databases such as ChEMBL [32, 33] and ChEBI [34, 35]. This approach enabled consistent compound mappings across datasets, with PubChem identifiers adopted as the preferred standard due to their extensive coverage [36–38]. Through this standardization process, 2,508 redundant compound IDs were identified and resolved.

**Disease mapping** For disease entity standardization, we leveraged the Human Disease Ontology database [39, 40], which provides comprehensive cross-referencing between Disease Ontology (DOID), Medical Subject Headings (MeSH), and Online Mendelian Inheritance in Man (OMIM) identifier systems. Through this standardization process, 118 redundant compound IDs were identified and resolved.

**Gene mapping** Genes are identified using the NCBI ID. However, genes retrieved from the DrugBank database may not have a corresponding NCBI ID. To preserve the information carried by such genes, we retained the DrugBank ID for 62 genes for which no mapping was possible.

### 2.5 Removal of duplicates

The steps described above aim to map the largest possible number of entities and interactions to a standardized space, allowing the identification of redundant information. To ensure data consistency, we checked for duplicate edges. In the first stage, exact duplicate triplets are identified and eliminated. However, due to the possibility that certain relationships are recorded with the head and tail nodes in reversed order, an additional step is required. Taking this into account, duplicate entries are detected and removed. The de-duplication procedure resulted in the elimination of 842,262 duplicate rows, thereby significantly improving the structural integrity and consistency of the graph.

### 2.6 Additional cleaning procedures

In the original DRKG, pathway nodes presented several inconsistencies across the various data sources used. Therefore, we initially removed all pathway nodes and their associated connections from the graphs. In Section 3.1, we will describe how this information was integrated back into the knowledge graph in a consistent manner. Finally, as an additional cleaning step, nodes representing Taxonomy and Symptoms were removed from the graph, as they were each linked to only a single entity and thus did not contribute additional meaningful information to the knowledge graph. The output of the proposed cleaning pipeline is a refined knowledge graph, free from redundancy, noise, and ambiguous informational content. This intermediate representation serves as a foundational stone for the construction of VITAGRAPH, incorporating node features derived and systematically processed from supplementary data sources, as described in the next session.

### 3 Enlarging the scope: toward VITAGRAPH

A hallmark of our dataset lies in its integration of additional data sources as well as the definition of biologically meaningful and expressive features. On the one hand, we augment the information content by adding pathway and drug-side effect information from new databases. On the other hand, we enrich the graph nodes with features. Drawing from both biological and chemical domains, the nodes within the graph are endowed with a comprehensive set of descriptors that capture their biochemical significance and role in the biological knowledge. This design paradigm ensures that, beyond the relational structure of the graph, the intrinsic properties of the individual entities contribute substantively to graph learning processes for biological tasks. This enriches the graph structure, leading to VITAGRAPH, a new, more comprehensive, and expressive knowledge graph for life science-centered machine learning and network science.

#### 3.1 Pathways

As mentioned in Section 2.6, pathway nodes were removed due to inconsistencies. To compensate for this, we chose to rely on a single, widely recognized and adopted database: Reactome [41, 42]. Subsequently, we introduced 2,153 new pathway nodes into the graph and connected them to the genes involved in those pathways with 68,380 edges, as detailed in the Reactome database. This resulted in a more consistent and unambiguous integration of molecular pathway knowledge within the graph.

#### 3.2 Drug-side effect information

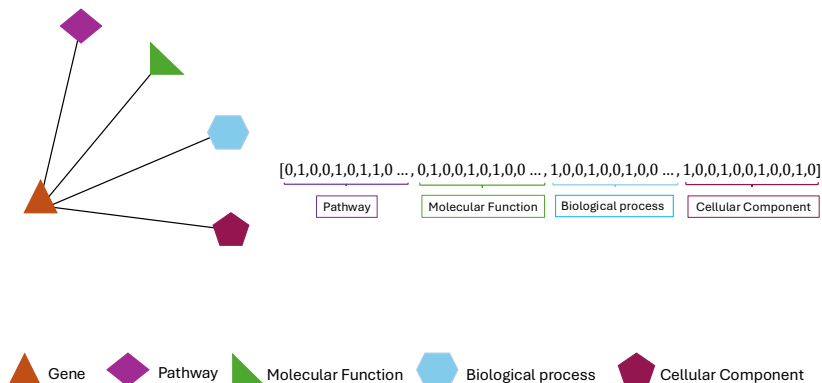
Given the relevance of predicting the side effects of a compound, we integrated the OnSIDES dataset [43] for compound-side effect edges. OnSIDES, curated from real-world pharmacovigilance data, offers a rich source of high-confidence associations that complement existing resources. By incorporating it, we aim to broaden the coverage of known adverse drug reactions, thereby supporting downstream research and analysis with a more comprehensive foundation of pharmacological knowledge. We incorporated the latest version of the dataset, v3.0.0, and selected only the highest-confidence set of edges. To ensure data consistency and avoid introducing noise, we included only those edges involving compounds already present in our graph. Additionally, we mapped and standardized compound and side effect identifiers to prevent redundancy. As a result, a total of 339,867 edges were integrated into the dataset.

#### 3.3 Elimination of compounds without SMILES representations

Accurate chemical representation is essential for computational analyses involving molecular compounds. SMILES (Simplified Molecular Input Line Entry System) strings [44] offer a standardized format for describing chemical structures. In this stage, the dataset was cross-referenced with a comprehensive compound dictionary incorporating SMILES annotations curated from DrugBank, GNBR, Hetionet, IntAct, DGIdb, and PubChem. Entries corresponding to compounds lacking an associated SMILES representation were excluded. Such compounds are typically either no longer available (e.g., withdrawn from the market) or proprietary in nature, with undisclosed chemical structures. Consequently, these entries were removed to maintain the openness and reproducibility of research. Moreover, SMILES representations are necessary for subsequent processing steps, such as the generation of Morgan fingerprints (see later), and this led to retaining only those compounds suitable for structural analysis. This filtering process eliminated 3,872 compounds and 239,219 edges.

#### 3.4 Morgan fingerprint generation

To further augment the chemical information content of the knowledge graph, compound nodes were associated with their corresponding Morgan fingerprints [45, 46]. Morgan fingerprints are a type of circular fingerprint that captures the local structural features of a molecule. By iteratively examining atomic neighborhoods within a defined radius, these fingerprints translate substructural characteristics into fixed-length binary vectors, where each bit denotes the presence (1) or absence (0) of a particular molecular feature. This representation is particularly valuable for similarity searches and machine learning applications in chemoinformatics. Each compound node was assigned a fingerprint feature vector of length 2,048, as is common in the field for machine representation



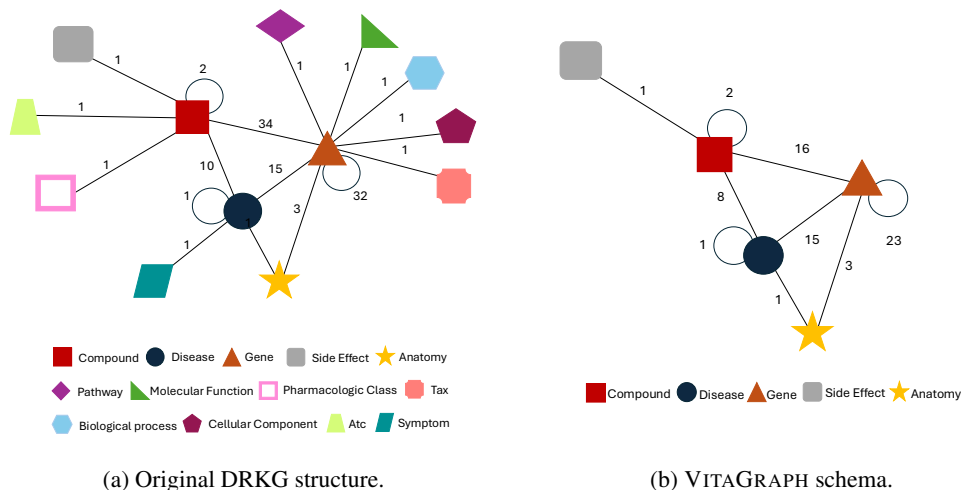


Figure 2: Comparison of the original DRKG and the new VITAGRAPH schema. In VITAGRAPH schema only a limited number of node and edge types are preserved, augmenting the coherence and reducing the noise within the graph.

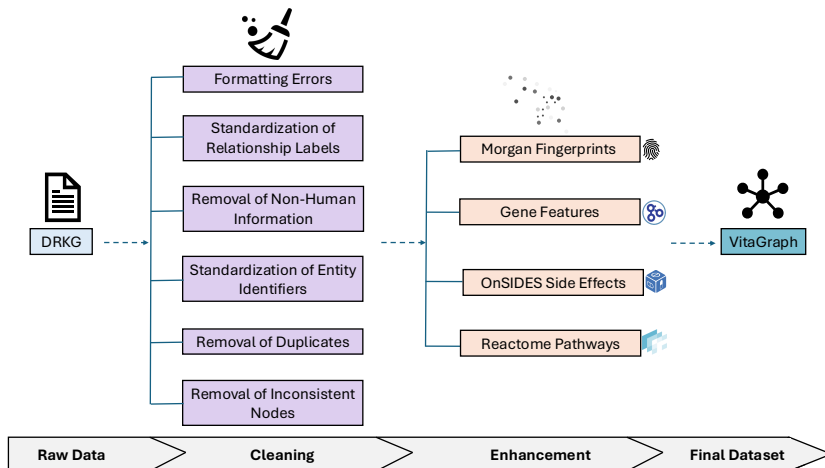


Figure 3: VITAGRAPH creation pipeline.

serve as strong benchmarks for assessing the utility and generalizability of knowledge graph-based representations in biomedical applications.

To rigorously assess the impact of our dataset enhancements, we performed experiments across three distinct versions of the dataset: (1) the original DRKG dataset, which serves as a baseline, (2) a cleaned version of DRKG including the Reactome and OnSIDES merge without the addition of the features presented in Section 3, and (3) the finally proposed VITAGRAPH, which includes both the cleaned structure and node features. This comparative setup allows us to isolate and quantify the contributions of data cleaning and feature enrichment to the predictive performance of the model.

#### 4.1 Model architectures

As baseline models, we employed modified versions of the relational graph convolutional network (R-GCN) [48] and composition-based multi-relational graph convolutional networks (CompGCN) [49], which were adapted to learn from heterogeneous multi-relational graph data. Those architectures are well-suited to the goals of our study, as they can exploit the complex relational structure of biomedical knowledge graphs like ours. Moreover, their flexibility in handling heterogeneous data makes it capable of learning from nodes that possess varying sets of features. To extend the baselines

to support heterogeneous nodes, we introduced a node-type-specific linear transformation prior to the graph convolution operations. This preprocessing step projects the feature vectors of different node types into a shared latent space to enable message passing across heterogeneous node types during training. Details on the experimental setup and hyperparameter optimization are provided in Appendix B.

## 4.2 Training setup

To train the model on different tasks, specific subsets of triplets were selected. For the PPI task, we used edges connecting pairs of gene entities. For the drug repurposing task, we used edges between compound and gene entities. Finally, for the side effect prediction task, we used edges linking compounds to side effects. While the loss is computed only on these task-specific subsets, all other edges remain in the graph to support message passing and information flow. We adopted a split of 70% training, 10% validation, and 20% test based on the target triplets for each task.

## 4.3 Results

In this section, we present and analyze the results obtained from our experimental setup. Tables 1, 2, 3 report the performance of the models across the various dataset versions and task configurations.

Table 1: Drug repurposing results.

Dataset	Model	AUROC	AUPRC	MRR	Hits@1	Hits@3	Hits@10
DRKG	R-GCN	0.914 $\pm$ 0.030	0.896 $\pm$ 0.028	0.148 $\pm$ 0.035	0.000 $\pm$ 0.000	0.025 $\pm$ 0.075	0.650 $\pm$ 0.166
	CompGCN	0.904 $\pm$ 0.023	0.881 $\pm$ 0.028	0.246 $\pm$ 0.093	<b>0.075 <math>\pm</math> 0.115</b>	0.350 $\pm$ 0.166	0.550 $\pm$ 0.187
VITAGRAPH (no feat)	R-GCN	<b>0.928 <math>\pm</math> 0.004</b>	<b>0.917 <math>\pm</math> 0.007</b>	0.176 $\pm$ 0.090	0.000 $\pm$ 0.000	0.175 $\pm$ 0.195	0.475 $\pm$ 0.305
	CompGCN	0.827 $\pm$ 0.077	0.796 $\pm$ 0.067	0.209 $\pm$ 0.121	0.050 $\pm$ 0.150	0.150 $\pm$ 0.166	0.675 $\pm$ 0.225
VITAGRAPH	R-GCN	0.887 $\pm$ 0.060	0.870 $\pm$ 0.053	0.219 $\pm$ 0.126	0.050 $\pm$ 0.100	0.250 $\pm$ 0.354	0.825 $\pm$ 0.160
	CompGCN	0.923 $\pm$ 0.013	0.901 $\pm$ 0.016	<b>0.257 <math>\pm</math> 0.046</b>	0.050 $\pm$ 0.100	<b>0.400 <math>\pm</math> 0.122</b>	<b>0.925 <math>\pm</math> 0.160</b>

Table 2: Compound-side effect results.

Dataset	Model	AUROC	AUPRC	MRR	Hits@1	Hits@3	Hits@10
DRKG	R-GCN	0.881 $\pm$ 0.024	0.839 $\pm$ 0.034	0.126 $\pm$ 0.136	0.050 $\pm$ 0.150	0.050 $\pm$ 0.150	0.300 $\pm$ 0.187
	CompGCN	0.870 $\pm$ 0.025	0.829 $\pm$ 0.025	0.158 $\pm$ 0.144	0.050 $\pm$ 0.150	0.150 $\pm$ 0.200	0.300 $\pm$ 0.384
VITAGRAPH (no feat)	R-GCN	<b>0.899 <math>\pm</math> 0.021</b>	<b>0.846 <math>\pm</math> 0.024</b>	<b>0.358 <math>\pm</math> 0.222</b>	<b>0.250 <math>\pm</math> 0.250</b>	<b>0.325 <math>\pm</math> 0.251</b>	<b>0.500 <math>\pm</math> 0.316</b>
	CompGCN	0.865 $\pm$ 0.027	0.807 $\pm$ 0.025	0.150 $\pm$ 0.112	0.000 $\pm$ 0.000	0.200 $\pm$ 0.350	0.350 $\pm$ 0.339
VITAGRAPH	R-GCN	0.888 $\pm$ 0.019	0.827 $\pm$ 0.023	0.326 $\pm$ 0.190	0.200 $\pm$ 0.245	<b>0.325 <math>\pm</math> 0.225</b>	0.475 $\pm$ 0.261
	CompGCN	0.824 $\pm$ 0.052	0.776 $\pm$ 0.043	0.134 $\pm$ 0.069	0.000 $\pm$ 0.000	0.125 $\pm$ 0.168	0.450 $\pm$ 0.245

Table 3: PPI results.

Dataset	Model	AUROC	AUPRC	MRR	Hits@1	Hits@3	Hits@10
DRKG	R-GCN	0.885 $\pm$ 0.032	0.871 $\pm$ 0.029	0.157 $\pm$ 0.085	0.050 $\pm$ 0.100	0.100 $\pm$ 0.122	0.500 $\pm$ 0.274
	CompGCN	<b>0.924 <math>\pm</math> 0.038</b>	<b>0.914 <math>\pm</math> 0.041</b>	0.245 $\pm$ 0.263	0.125 $\pm$ 0.301	<b>0.275 <math>\pm</math> 0.325</b>	<b>0.600 <math>\pm</math> 0.300</b>
VITAGRAPH (no feat)	R-GCN	0.893 $\pm$ 0.074	0.890 $\pm$ 0.069	<b>0.280 <math>\pm</math> 0.204</b>	<b>0.175 <math>\pm</math> 0.225</b>	<b>0.275 <math>\pm</math> 0.261</b>	0.575 $\pm$ 0.354
	CompGCN	0.859 $\pm$ 0.041	0.845 $\pm$ 0.039	0.150 $\pm$ 0.055	0.000 $\pm$ 0.000	0.100 $\pm$ 0.200	0.475 $\pm$ 0.261
VITAGRAPH	R-GCN	0.859 $\pm$ 0.059	0.852 $\pm$ 0.054	0.139 $\pm$ 0.069	0.025 $\pm$ 0.075	0.125 $\pm$ 0.168	0.475 $\pm$ 0.325
	CompGCN	0.884 $\pm$ 0.061	0.882 $\pm$ 0.059	0.180 $\pm$ 0.141	0.075 $\pm$ 0.160	0.075 $\pm$ 0.160	0.475 $\pm$ 0.284

At first glance, the results on the original DRKG appear promising. However, upon deeper inspection, we demonstrate that these results are significantly affected by data leakage between the training, validation, and test sets.

To identify potential leakage, we examined the three dataset splits by checking for overlap in three ways: 1) duplicate identification, 2) relation-level redundancy, and 3) entity-level redundancy. With the first approach, we searched for identical triplets across splits, including their inverse forms (e.g.,



if A interacts with B is in the training set, and B interacts with A appears in the test set). This directly indicates leakage of connectivity information. With the second, we apply the pipeline’s relation standardization across the splits and check for overlaps. In the original dataset, the same semantic interaction can be represented by multiple redundant relation IDs. Although these IDs are different, they retain the same structural information. As a result, even if a relation appears with a different name in the test set, the model may still recognize and exploit its topology learned from the training set. By standardizing relations, we can identify overlapping interactions that reveal this type of data leakage. Finally, for entity-level redundancy, we standardized entities across splits to detect duplicate nodes. In the original dataset, the same entity may be duplicated under different IDs. These redundant entities typically share similar latent representations and have overlapping neighborhoods. We consider it a form of leakage when an edge is masked for a node in the test set, but the same edge is unmasked for a redundant node in the training set. In this scenario, the model can infer the missing edge based on the connections of a nearly identical redundant entity’s latent representation. Table 4 quantifies the extent of data leakage across tasks. We find substantial leakage in the PPI task and the drug repurposing task, significantly compromising the reliability of the results. In contrast, the side effect prediction task remains unaffected. This is because its edges—which connect compounds to side effects—all originate from the same source dataset (SIDER) and are not subject to redundancy.

Table 4: Leakage interaction ratios for train/val and train/test splits. No leakage is present for the compound–side effect task.

Split	PPI	Drug repurposing	Compound-side effect
Train Val	$0.655 \pm 0.002$	$0.182 \pm 0.003$	–
Train Test	$0.655 \pm 0.001$	$0.187 \pm 0.002$	–

The results show that our approach achieves performance comparable to, or better than, the original dataset. However, a fair comparison is not possible due to the substantial data leakage present in the original dataset. Constructing a leakage-free version of that dataset would result in a structure very similar to our proposed version, albeit without the additional enrichment we introduce.

## 5 Conclusions

In this work, we introduce VITAGRAPH, a knowledge graph specifically designed to support graph machine learning in biologically and chemically relevant applications. Building upon the DRKG, we perform comprehensive data cleaning and node enrichment by incorporating biochemically meaningful features derived from diverse data sources. The resulting knowledge graph is intended to serve the research community in the discovery of novel biological insights, such as previously unidentified gene–gene interactions or drug repurposing opportunities, treated as link prediction problems. Our results demonstrate that relational graph neural network models can effectively learn from VITAGRAPH, indicating its suitability as a benchmark for graph machine learning and knowledge extraction models. Moreover, novel connections discovered through this framework, once experimentally validated, can be reintegrated into the graph, thereby continually enhancing the breadth and depth of biomedical knowledge it contains. One limitation of our dataset lies in its reliance on the quality of the integrated data sources. Nevertheless, by maintaining regular updates, we aim to provide researchers with a reliable and continually improving resource for biomedical discovery.

## References

- [1] Bertil Schmidt and Andreas Hildebrandt. From gpus to ai and quantum: three waves of acceleration in bioinformatics. *Drug Discovery Today*, page 103990, 2024.
- [2] Yasset Perez-Riverol, Mingze Bai, Felipe da Veiga Leprevost, Silvano Squizzato, Young Mi Park, Kenneth Haug, Adam J Carroll, Dylan Spalding, Justin Paschall, Mingxun Wang, et al. Discovering and linking public omics data sets using the omics discovery index. *Nature biotechnology*, 35(5):406–409, 2017.
- [3] Yasset Perez-Riverol, Andrey Zorin, Gaurhari Dass, Manh-Tu Vu, Pan Xu, Mihai Glont, Juan Antonio Vizcaíno, Andrew F Jarnuczak, Robert Petryszak, Peipei Ping, et al. Quantifying the impact of public omics data. *Nature communications*, 10(1):3512, 2019.
- [4] Albert-László Barabási, Natali Gulbahce, and Joseph Loscalzo. Network medicine: a network-based approach to human disease. *Nature reviews genetics*, 12(1):56–68, 2011.
- [5] Rose Oughtred, Jennifer Rust, Christie Chang, Bobby-Joe Breitkreutz, Chris Stark, Andrew Willems, Lorrie Boucher, Genie Leung, Nadine Kolas, Frederick Zhang, et al. The biogrid database: A comprehensive biomedical resource of curated protein, genetic, and chemical interactions. *Protein Science*, 30(1):187–200, 2021.
- [6] Damian Szklarczyk, Rebecca Kirsch, Mikaela Koutrouli, Katerina Nastou, Farrokh Mehryary, Radja Hachilif, Annika L Gable, Tao Fang, Nadezhda T Doncheva, Sampo Pyysalo, et al. The string database in 2023: protein–protein association networks and functional enrichment analyses for any sequenced genome of interest. *Nucleic acids research*, 51(D1):D638–D646, 2023.
- [7] Katja Luck, Dae-Kyum Kim, Luke Lambourne, Kerstin Spirohn, Bridget E Begg, Wenting Bian, Ruth Brignall, Tiziana Cafarelli, Francisco J Campos-Laborie, Benoit Charlotiaux, et al. A reference map of the human binary protein interactome. *Nature*, 580(7803):402–408, 2020.
- [8] Saket Navlakha and Carl Kingsford. The power of protein interaction networks for associating genes with diseases. *Bioinformatics*, 26(8):1057–1063, 2010.
- [9] Paola Stolfi, Andrea Mastropietro, Giuseppe Pasculli, Paolo Tieri, and Davide Vergni. Niapu: network-informed adaptive positive-unlabeled learning for disease gene identification. *Bioinformatics*, 39(2):btac848, 2023.
- [10] Andrea Mastropietro, Gianluca De Carlo, and Aris Anagnostopoulos. Xgdag: explainable gene–disease associations via graph neural networks. *Bioinformatics*, 39(8):btad482, 2023.
- [11] Lun Hu, Xiaojuan Wang, Yu-An Huang, Pengwei Hu, and Zhu-Hong You. A survey on computational models for predicting protein–protein interactions. *Briefings in bioinformatics*, 22(5):bbab036, 2021.
- [12] Pau Badia-i Mompel, Lorna Wessels, Sophia Müller-Dott, Rémi Trimbou, Ricardo O Ramirez Flores, Ricard Argelaguet, and Julio Saez-Rodriguez. Gene regulatory network inference in the era of single-cell multi-omics. *Nature Reviews Genetics*, 24(11):739–754, 2023.
- [13] Janet Piñero, Àlex Bravo, Núria Queralt-Rosinach, Alba Gutiérrez-Sacristán, Jordi Deu-Pons, Emilio Centeno, Javier García-García, Ferran Sanz, and Laura I Furlong. Disgenet: a comprehensive platform integrating information on human disease-associated genes and variants. *Nucleic acids research*, page gkw943, 2016.
- [14] Janet Piñero, Juan Manuel Ramírez-Angueta, Josep Saüch-Pitarch, Francesco Ronzano, Emilio Centeno, Ferran Sanz, and Laura I Furlong. The disgenet knowledge platform for disease genomics: 2019 update. *Nucleic acids research*, 48(D1):D845–D855, 2020.
- [15] Craig Knox, Mike Wilson, Christen M Klinger, Mark Franklin, Eponine Oler, Alex Wilson, Allison Pon, Jordan Cox, Na Eun Chin, Seth A Strawbridge, et al. Drugbank 6.0: the drugbank knowledgebase for 2024. *Nucleic acids research*, 52(D1):D1265–D1275, 2024.

- [16] Allan Peter Davis, Cynthia J Grondin, Robin J Johnson, Daniela Sciaky, Benjamin L King, Roy McMorran, Jolene Wieggers, Thomas C Wieggers, and Carolyn J Mattingly. The comparative toxicogenomics database: update 2017. *Nucleic acids research*, 45(D1):D972–D978, 2017.
- [17] Michael Kuhn, Ivica Letunic, Lars Juhl Jensen, and Peer Bork. The sider database of drugs and side effects. *Nucleic acids research*, 44(D1):D1075–D1079, 2016.
- [18] Nicholas P Tatonetti, Patrick P Ye, Roxana Daneshjou, and Russ B Altman. Data-driven prediction of drug effects and interactions. *Science translational medicine*, 4(125):125ra31–125ra31, 2012.
- [19] Pablo Perdomo-Quinteiro and Alberto Belmonte-Hernández. Knowledge graphs for drug repurposing: a review of databases and methods. *Briefings in Bioinformatics*, 25(6):bbae461, 2024.
- [20] Tiffany J Callahan, Ignacio J Tripodi, Adrianne L Stefanski, Luca Cappelletti, Sanya B Taneja, Jordan M Wyrwa, Elena Casiraghi, Nicolas A Matentzoglou, Justin Reese, Jonathan C Silverstein, et al. An open source knowledge graph ecosystem for the life sciences. *Scientific Data*, 11(1):363, 2024.
- [21] Vassilis N. Ioannidis, Xiang Song, Saurav Manchanda, Mufei Li, Xiaoqin Pan, Da Zheng, Xia Ning, Xiangxiang Zeng, and George Karypis. Drkg - drug repurposing knowledge graph for covid-19. <https://github.com/gnn4dr/DRKG/>, 2020.
- [22] Vassilis N Ioannidis, Da Zheng, and George Karypis. Few-shot link prediction via graph neural networks for covid-19 drug-repurposing. *arXiv preprint arXiv:2007.10261*, 2020.
- [23] Md Kamrul Islam, Diego Amaya-Ramirez, Bernard Maigret, Marie-Dominique Devignes, Sabeur Aridhi, and Malika Smaïl-Tabbone. Molecular-evaluated and explainable drug repurposing for covid-19 using ensemble knowledge graph embedding. *Scientific Reports*, 13(1):3643, 2023.
- [24] David S Wishart, Craig Knox, An Chi Guo, Dean Cheng, Savita Shrivastava, Dan Tzur, Bijaya Gautam, and Murtaza Hassanali. Drugbank: a knowledgebase for drugs, drug actions and drug targets. *Nucleic acids research*, 36(suppl\_1):D901–D906, 2008.
- [25] Daniel Scott Himmelstein, Antoine Lizee, Christine Hessler, Leo Brueggeman, Sabrina L Chen, Dexter Hadley, Ari Green, Pouya Khankhanian, and Sergio E Baranzini. Systematic integration of biomedical knowledge prioritizes drugs for repurposing. *elife*, 6:e26726, 2017.
- [26] Bethany Percha and Russ B Altman. A global network of biomedical relationships derived from text. *Bioinformatics*, 34(15):2614–2624, 2018.
- [27] Noemi Del Toro, Anjali Shrivastava, Eliot Ragueneau, Birgit Meldal, Colin Combe, Elisabet Barrera, Livia Perfetto, Karyn How, Prashansa Ratan, Gautam Shirodkar, et al. The intact database: efficient access to fine-grained molecular interaction data. *Nucleic acids research*, 50(D1):D648–D653, 2022.
- [28] Malachi Griffith, Obi L Griffith, Adam C Coffman, James V Weible, Josh F McMichael, Nicholas C Spies, James Koval, Indrani Das, Matthew B Callaway, James M Eldred, et al. Dgidb: mining the druggable genome. *Nature methods*, 10(12):1209–1210, 2013.
- [29] Matthew Cannon, James Stevenson, Kathryn Stahl, Rohit Basu, Adam Coffman, Susanna Kiwala, Joshua F McMichael, Kori Kuzma, Dorian Morrissey, Kelsy Cotto, et al. Dgidb 5.0: rebuilding the drug–gene interaction database for precision medicine and drug discovery platforms. *Nucleic acids research*, 52(D1):D1227–D1235, 2024.
- [30] Michael Ashburner, Catherine A Ball, Judith A Blake, David Botstein, Heather Butler, J Michael Cherry, Allan P Davis, Kara Dolinski, Selina S Dwight, Janan T Eppig, et al. Gene ontology: tool for the unification of biology. *Nature genetics*, 25(1):25–29, 2000.
- [31] Jon Chambers, Mark Davies, Anna Gaulton, Anne Hersey, Sameer Velankar, Robert Petryszak, Janna Hastings, Louisa Bellis, Shaun McGlinchey, and John P Overington. Unichem: a unified chemical structure cross-referencing and identifier tracking system. *Journal of cheminformatics*, 5(1):3, 2013.

- [32] Anna Gaulton, Louisa J Bellis, A Patricia Bento, Jon Chambers, Mark Davies, Anne Hersey, Yvonne Light, Shaun McGlinchey, David Michalovich, Bissan Al-Lazikani, et al. ChEMBL: a large-scale bioactivity database for drug discovery. *Nucleic acids research*, 40(D1):D1100–D1107, 2012.
- [33] Barbara Zdrazil, Eloy Felix, Fiona Hunter, Emma J Manners, James Blackshaw, Sybilla Corbett, Marleen de Veij, Harris Ioannidis, David Mendez Lopez, Juan F Mosquera, et al. The ChEMBL database in 2023: a drug discovery platform spanning multiple bioactivity data types and time periods. *Nucleic acids research*, 52(D1):D1180–D1192, 2024.
- [34] Kirill Degtyarenko, Paula De Matos, Marcus Ennis, Janna Hastings, Martin Zbinden, Alan McNaught, Rafael Alcántara, Michael Darsow, Mickaël Guedj, and Michael Ashburner. ChEBI: a database and ontology for chemical entities of biological interest. *Nucleic acids research*, 36 (suppl\_1):D344–D350, 2007.
- [35] Janna Hastings, Gareth Owen, Adriano Dekker, Marcus Ennis, Namrata Kale, Venkatesh Muthukrishnan, Steve Turner, Neil Swainston, Pedro Mendes, and Christoph Steinbeck. ChEBI in 2016: Improved services and an expanding collection of metabolites. *Nucleic acids research*, 44(D1):D1214–D1219, 2016.
- [36] Evan E Bolton, Yanli Wang, Paul A Thiessen, and Stephen H Bryant. Pubchem: integrated platform of small molecules and biological activities. In *Annual reports in computational chemistry*, volume 4, pages 217–241. Elsevier, 2008.
- [37] Qingliang Li, Tiejun Cheng, Yanli Wang, and Stephen H Bryant. Pubchem as a public resource for drug discovery. *Drug discovery today*, 15(23-24):1052–1057, 2010.
- [38] Sunghwan Kim, Jie Chen, Tiejun Cheng, Asta Gindulyte, Jia He, Siqian He, Qingliang Li, Benjamin A Shoemaker, Paul A Thiessen, Bo Yu, et al. Pubchem 2025 update. *Nucleic Acids Research*, 53(D1):D1516–D1525, 2025.
- [39] Lynn M Schriml, Elvira Mitraka, James Munro, Becky Tauber, Mike Schor, Lance Nickle, Victor Felix, Linda Jeng, Cynthia Bearer, Richard Lichenstein, et al. Human disease ontology 2018 update: classification, content and workflow expansion. *Nucleic acids research*, 47(D1):D955–D962, 2019.
- [40] Lynn M Schriml, James B Munro, Mike Schor, Dustin Olley, Carrie McCracken, Victor Felix, J Allen Baron, Rebecca Jackson, Susan M Bello, Cynthia Bearer, et al. The human disease ontology 2022 update. *Nucleic acids research*, 50(D1):D1255–D1261, 2022.
- [41] Imre Vastrik, Peter D’Eustachio, Esther Schmidt, Geeta Joshi-Tope, Gopal Gopinath, David Croft, Bernard de Bono, Marc Gillespie, Bijay Jassal, Suzanna Lewis, et al. Reactome: a knowledge base of biologic pathways and processes. *Genome biology*, 8:1–13, 2007.
- [42] Marija Milacic, Deidre Beavers, Patrick Conley, Chuqiao Gong, Marc Gillespie, Johannes Griss, Robin Haw, Bijay Jassal, Lisa Matthews, Bruce May, et al. The reactome pathway knowledgebase 2024. *Nucleic acids research*, 52(D1):D672–D678, 2024.
- [43] Yutaro Tanaka, Hsin Yi Chen, Pietro Belloni, Undina Gisladdottir, Jenna Kefeli, Jason Patterson, Apoorva Srinivasan, Michael Zietz, Gaurav Sirdeshmukh, Jacob Berkowitz, et al. OnSides database: Extracting adverse drug events from drug labels using natural language processing models. *Med*, 2025.
- [44] David Weininger. Smiles, a chemical language and information system. 1. introduction to methodology and encoding rules. *Journal of Chemical Information and Computer Sciences*, 28 (1):31–36, 1988.
- [45] Harry L. Morgan. The generation of a unique machine description for chemical structures—a technique developed at chemical abstracts service. *Journal of Chemical Documentation*, 5(2): 107–113, 1965.
- [46] David Rogers and Mathew Hahn. Extended-connectivity fingerprints. *Journal of Chemical Information and Modeling*, 50(5):742–754, 2010.

- [47] Alice Capecchi, Daniel Probst, and Jean-Louis Reymond. One molecular fingerprint to rule them all: drugs, biomolecules, and the metabolome. *Journal of cheminformatics*, 12:1–15, 2020.
- [48] Michael Schlichtkrull, Thomas N Kipf, Peter Bloem, Rianne Van Den Berg, Ivan Titov, and Max Welling. Modeling relational data with graph convolutional networks. In *The semantic web: 15th international conference, ESWC 2018, Heraklion, Crete, Greece, June 3–7, 2018, proceedings 15*, pages 593–607. Springer, 2018.
- [49] Shikhar Vashishth, Soumya Sanyal, Vikram Nitin, and Partha Talukdar. Composition-based multi-relational graph convolutional networks. *arXiv preprint arXiv:1911.03082*, 2019.

## A Details on VITAGRAPH structure

Table 5 shows the mapping between the interaction types in VITAGRAPH and the original DRKG with the corresponding sources. Tables 6 and 7 illustrate details on the data sources for edge and nodes, respectively.

Table 5: Mapping of interaction types to their corresponding database sources. Each row corresponds to a unified relation type, while the columns indicate the presence or absence of that relation in the original source databases, with the corresponding interaction name if that interaction is present. For example, the edge types labeled “Activator” and “Agonist” from the DGIdb dataset are consolidated into a single standardized Activator relation type in our dataset. A dash (“-”) denotes that the corresponding interaction type is not present in the given data source (\*DrugHumGen, \*\*HumGenHumGen).

New interaction	DrugBank	GNBR	Hetionet	STRING	IntAct	DGIdb	bioarx
Activator	-	A+	-	-	-	Activator Agonist	-
Blocker	-	A-	-	-	-	Antagonist, Blocker, Channel Blocker	-
CMP_BIND	Target	B	CbG	-	Direct Interaction, Association, Physical Interaction	Binder	DHG*
ENZYME	Enzyme	Z	-	-	-	-	-
EXPRESSION	-	E	-	Expression	-	-	-
Regulation	-	Rg	Gr>G	-	-	-	-
UPREGULATION	-	E+	CuG	-	-	-	-
DOWNREGULATION	-	E-, N	CdG	-	-	Inhibitor	-
GENE_BIND	-	B	GiG	Binding	Physical Assoc., Assoc., Dir. Int.	-	HGHG**
TREATMENT	Treats	T	CtD	-	-	-	-
J_c	-	J	-	-	-	-	-
J_g	-	J	-	-	-	-	-
gene_OTHER_cmp	-	-	-	-	-	Other	-
gene_OTHER_gene	-	-	-	Other	-	-	-

## B Experimental Setup

To produce a fair comparison of our baselines, we made sure to find the optimal parameters for each combination of task and dataset. The experiments were carried out using 4 NVIDIA A40 GPUs with 48 GB of VRAM. The hyperparameter tuning to around one week of computation. The experiments shown in the main paper took around 48 hours of computation.

Our search grid included the following parameters:

- Linear layer size: 5, 10, 20, 30, 40
- Convolutional layer: 1, 2
- First convolutional layer size: 5, 10, 15, 20
- Second convolutional layer size: 5, 10

Table 6: Edge type to source.

Relation	DGIDb	DrugBank	GNBR	Hetionet	IntAct	OnSIDES	STRING	bioarx	Total
Anatomy–Gene	0	0	0	726 156	0	0	0	0	726 156
Compound–Compound	0	1 161 176	0	6 441	0	0	0	0	1 167 617
Compound–Disease	0	4 502	68 455	609	0	0	0	0	73 566
Compound–Gene	22 750	8 671	34 469	41 751	1 563	0	0	24 248	133 452
Compound–SideEffect	0	0	0	138 017	0	284 235	0	0	422 252
Disease–Anatomy	0	0	0	3 602	0	0	0	0	3 602
Disease–Disease	0	0	0	543	0	0	0	0	543
Disease–Gene	0	0	65 679	27 936	0	0	0	458	94 073
Disease–Symptom	0	0	0	3 357	0	0	0	0	3 357
Gene–Gene	0	0	23 994	461 263	141 926	0	723 259	29 523	1 379 965
<b>Total</b>	22 750	1 174 349	192 597	1 409 675	143 489	284 235	723 259	54 229	4 004 583

Table 7: Node type to source.

Source	Anatomy	Compound	Disease	Gene	SideEffect	Symptom	Total
CHEBI	0	176	0	0	0	0	176
ChEMBL	0	77	0	0	0	0	77
DOID	0	0	2 390	0	0	0	2 390
MESH	0	0	2 356	0	0	415	2 771
NCBI	0	0	0	20 844	0	0	20 844
OMIM	0	0	31	0	0	0	31
PubChem_Compounds	0	15 302	0	0	0	0	15 302
UBERON	400	0	0	0	0	0	400
bioarx	0	0	27	0	0	0	27
drugbank	0	0	0	62	0	0	62
molport	0	221	0	0	0	0	221
umls	0	0	0	0	5 704	0	5 704
zinc	0	53	0	0	0	0	53
<b>Total</b>	400	15 829	4 804	20 906	5 704	415	48 058

- Learning rate: 0.001, 0.01
- Regularization: 0.001, 0.01
- Number of bases: 4, 8, 16
- Epochs: 400
- Dropout: 0.1, 0.2, 0.3
- Operation type: subtraction, multiplication, circular correlation

The following tables from Table 8 through Table 16 list the parameters of the best models divided by task and the dataset used.

Table 8: Best hyperparameters side effect prediction in DRKG dataset.

Model	# Conv Layers	Conv_1 Size	Conv_2 Size	Linear Size	Learning Rate	# Bases	Dropout	Op Type	Regularization
R-GCN	2	40	15	30	0.01	32	–	–	0.001
R-GAT	2	15	10	40	0.01	4	–	–	0.001
CompGCN	1	5	-	40	0.01	–	0.3	mult	0.01

## C Data sources details

Our work is released under the Attribution-NonCommercial 4.0 International (CC BY-NC 4.0) license. However, due to data integration from diverse sources, the individual licenses of each data provider

Table 9: Best hyperparameters for side effect prediction in VITAGRAPH with no features.

Model	# Conv Layers	Conv_1 Size	Conv_2 Size	Linear Size	Learning Rate	# Bases	Dropout	Op Type	Regularization
R-GCN	1	10	-	30	0.01	8	–	–	0.001
R-GAT	1	5	-	40	0.01	8	–	–	0.001
CompGCN	1	15	-	5	0.001	–	0.2	sub	0.001

Table 10: Best hyperparameters for side effect prediction in VITAGRAPH.

Model	# Conv Layers	Conv_1 Size	Conv_2 Size	Linear Size	Learning Rate	# Bases	Dropout	Op Type	Regularization
R-GCN	2	10	5	40	0.01	16	–	–	0.001
R-GAT	1	10	-	5	0.01	4	–	–	0.001
CompGCN	1	20	-	40	0.001	–	0.2	sub	0.01

Table 11: Best hyperparameters for the prediction of PPI in DRKG.

Model	# Conv Layers	Conv_1 Size	Conv_2 Size	Linear Size	Learning Rate	# Bases	Dropout	Op Type	Regularization
R-GCN	1	10	-	50	0.01	16	–	–	0.1
R-GAT	1	15	-	10	0.01	4	–	–	0.01
CompGCN	1	15	-	30	0.01	–	0.1	mult	0.01

Table 12: Best hyperparameters for the prediction of PPI in VITAGRAPH with no features.

Model	# Conv Layers	Conv_1 Size	Conv_2 Size	Linear Size	Learning Rate	# Bases	Dropout	Op Type	Regularization
R-GCN	1	15	-	40	0.01	16	–	–	0.01
R-GAT	1	15	-	20	0.01	8	–	–	0.001
CompGCN	1	5	-	30	0.01	–	0.2	mult	0.001

Table 13: Best hyperparameters for the prediction of PPI in VITAGRAPH.

Model	# Conv Layers	Conv_1 Size	Conv_2 Size	Linear Size	Learning Rate	# Bases	Dropout	Op Type	Regularization
R-GCN	2	10	5	10	0.01	4	–	–	0.001
R-GAT	1	10	-	40	0.01	16	–	–	0.01
CompGCN	1	10	-	10	0.01	–	0.1	mult	0.001

Table 14: Best hyperparameters for drug repurposing in DRKG.

Model	# Conv Layers	Conv_1 Size	Conv_2 Size	Linear Size	Learning Rate	# Bases	Dropout	Op Type	Regularization
R-GCN	2	15	5	30	0.01	4	–	–	0.01
R-GAT	1	10	-	40	0.01	16	–	–	0.01
CompGCN	2	15	10	10	0.01	–	0.2	mult	0.001

Table 15: Best hyperparameters for drug repurposing in VITAGRAPH with no features.

Model	# Conv Layers	Conv_1 Size	Conv_2 Size	Linear Size	Learning Rate	# Bases	Dropout	Op Type	Regularization
R-GCN	1	10	-	20	0.01	4	–	–	0.001
R-GAT	1	10	-	40	0.01	16	–	–	0.01
CompGCN	1	5	-	5	0.01	–	0.3	mult	0.01



Table 16: Best hyperparameters for drug repurposing in VITAGRAPH.

Model	# Conv Layers	Conv_1 Size	Conv_2 Size	Linear Size	Learning Rate	# Bases	Dropout	Op Type	Regularization
R-GCN	1	5	-	30	0.001	8	–	–	0.01
R-GAT	1	20	-	30	0.01	16	–	–	0.01
CompGCN	1	15	-	20	0.01	–	0.3	sub	0.01

should be considered, applied on a per-node and per-edge basis, depending on the database of origin. We hereby list the sources used, along with their license:

- Reactome: Data are licensed under the Creative Commons Public Domain Dedication (CC0). More information at <https://reactome.org/license>
- OnSIDES: The dataset is licensed under the MIT License. The license details can be found in the GitHub repository: <https://github.com/tatonetti-lab/onsides>
- Hetionet: Hetionet original data is licensed under the Creative Commons Public Domain Dedication (CC0). More information at <https://github.com/hetio/hetionet>. For the data it integrates from additional external resources, the respective licenses are provided at <https://github.com/dhimmel/integrate/blob/master/licenses/README.md>
- UniChem: Data are licensed under the Creative Commons Public Domain Dedication (CC0). More information at <https://jcheminf.biomedcentral.com/articles/10.1186/1758-2946-5-3>.
- DRKG: The project is released under the Apache-2.0 License. Being itself an integration of several data sources, details on the licenses of the data it uses are available at <https://github.com/gnn4dr/DRKG/blob/master/licenses/Readme.md>